

Bubble Suppression on a High Lift Wing Section Using Synthetic Jet

Amsha S O N Ramesh* and N Balakrishnan**

**Indian Institute of Science*

Department of Aerospace Engineering, IISc, Bengaluru, 560012

amshas@iisc.ac.in · onr@iisc.ac.in · nbalak@iisc.ac.in

Abstract

A highly cambered fixed wing configuration aided with synthetic jet, as separation control device, is proposed as a viable candidate for Short distance Takeoff and Landing aircraft and studied. The test case of round synthetic jet in a cross-flow, is used to validate the dynamic mesh model for predicting the actuator driven flow. The hump model with oscillatory control is used for studying the effect of jet momentum and frequency in suppressing the bubble. The estimate of reduced frequencies and momentum coefficients for the expected pressure recovery has been found, and implemented in a representative configuration to understand the efficacy of the control device in suppressing flow separation and consequent enhancement in lift.

1. Introduction

Short distance Take-off and Landing (STOL) aircraft shows a lot of promise in future urban air mobility, enabling us to take-off from roads and under prepared runways. STOL aircrafts have less challenges in certification compared to vertical take-off and landing aircrafts because of their conformity to conventional design and better safety. The requirement of high coefficient of lift to take-off with a certain payload capacity at lower take-off speeds, calls for high lift sections. The complexity, cost and maintenance of such conventional multi-element sections can be significant and beyond the limits envisaged for low cost urban air mobility. Therefore, the proposal is to replace such a system with an optimized high cambered fixed wing configuration assisted by active control device to suppress flow separation to achieve the required lift. Further enhancement in lift may be realised by appropriately leveraging the propeller slipstream effects. Active flow control using synthetic jets is being considered for this purpose and forms the focus of the results presented in this work.

Synthetic jets are simple in design, constitutes a cavity with an opening to the receding boundary layer over the wing, and a piston as one of its interior walls which pumps the air in and out of the cavity, thus energizing the external flow. The interaction between the oscillating jet and the freestream flow is quite difficult to be modelled numerically given the evolution of complex coherent and turbulent structures. Therefore, it is imperative to adequately validate the CFD tools used in such simulations. Towards this goal, the published experimental data from the workshop on CFD Validation on Synthetic Jets and Turbulent Separation Control is made use of.¹ The flow evolution of synthetic jets and its interaction with external flow has been studied in details in many literature.^{2,3} The effect of adding synthetic jet to airfoil surfaces has proven to improve the aerodynamic efficiency.⁴⁻⁶

The objective of the work is to study and integrate the synthetic jet control system in the design of a high cambered wing section to achieve better aerodynamic efficiency. The validated CFD process is proposed to be used in all further simulations pertaining to the design of high-lift wing. Unsteady simulations are carried out using the Spalart Allmaras turbulence model.⁷ A study on control parameters affecting the suppression of separated flow in the standard hump model is carried out. Based on the results, the synthetic jet with selected control parameters are introduced to the new wing section and tested.

2. CFD validation of Hump Model with oscillatory control

The second test case from the workshop, a round synthetic jet in a crossflow,^{8,9} is used to validate the moving mesh strategy adapted to mimic the actuator motion. This case was studied earlier and excellent match with experimental data was observed.¹⁰ The dynamic mesh model is adopted to the hump with oscillatory jet control to study influence of control parameters in suppressing the separation bubble.

SYNTHETIC JET CONTROL

Experimental study has been conducted on wall-mounted two-dimensional hump with an actuator cavity for the zero-mass flux oscillatory control.^{11,12} The concave step creates a separation bubble downstream of the hump. A spanwise slot connected to an actuator cavity is provided at 65 percent of the chord. The chord length is approximately 420 mm. The baseline flow over the hump is at Mach number 0.1, has a freestream velocity of 34.6 m/s. The ambient pressure is 101325.15 Pa.

The experiments were conducted to understand the parameters affecting the control.¹² It was inferred that the control depends on a number of parameters including Reynolds number, the reduced frequency, reduced amplitude, the formation and interaction of coherent structures, surface pressure waves and other turbulence statistics. The reduced frequency, F^+ , and the jet momentum coefficient, C_μ for the incompressible oscillatory flow are defined as,

$$F^+ = \frac{f_e X}{U_\infty} \quad (1)$$

$$C_\mu = \frac{2b}{c} \frac{\overline{u_j^2}}{U_\infty^2} \quad (2)$$

where X is the distance from the slot to the baseline reattachment line, b is the slit width, c is the chord length, $\overline{u_j}$ is the periodic component of jet velocity, and U_∞ the freestream velocity as per the experimental paper. The flow over this hump at a fixed Reynolds number of interest is simulated to analyse the effect of reduced frequency and jet velocity amplitude in suppressing the bubble. Simulations were carried out for a range of F^+ and C_μ .

2.1 Solution Methodology

High resolution Flow solver on Unstructured meshes (HiFUN) is a highly scalable finite volume code optimized to solve aerodynamic problems in unstructured meshes.¹³ Roe scheme¹⁴ with linear solution reconstruction and Venkatakrishnan limiter¹⁵ are used for the inviscid flux calculation. The code employs matrix-free implicit Symmetric Gauss-Seidel iterations for convergence acceleration.¹⁶ Second order temporal accuracy is achieved using a standard BDF2 discretization within a dual time stepping framework.¹⁷ One equation eddy viscosity model by Spalart Allmaras⁷ is used to close the Reynolds Averaged Navier Stokes (RANS) equations for solving the turbulent flow.

Different methods have been used to study the synthetic jet actuators numerically in literature, including methods like unsteady velocity boundary conditions¹⁸ and dynamic mesh method like spring analogy.¹⁹ The actuator motion is represented using a cylinder-piston arrangement employing dynamic mesh movement strategy. The moving piston wall position is updated every time step based on a predefined motion. The new vertex locations in the cylinder domain are obtained by linearly redistributing the vertices along the direction of the piston displacement and the dynamic mesh algorithm is effected. This provides a reasonable framework in mimicking the motion of a vibrating diaphragm in a synthetic jet actuator.

2.2 Computational domain and mesh details

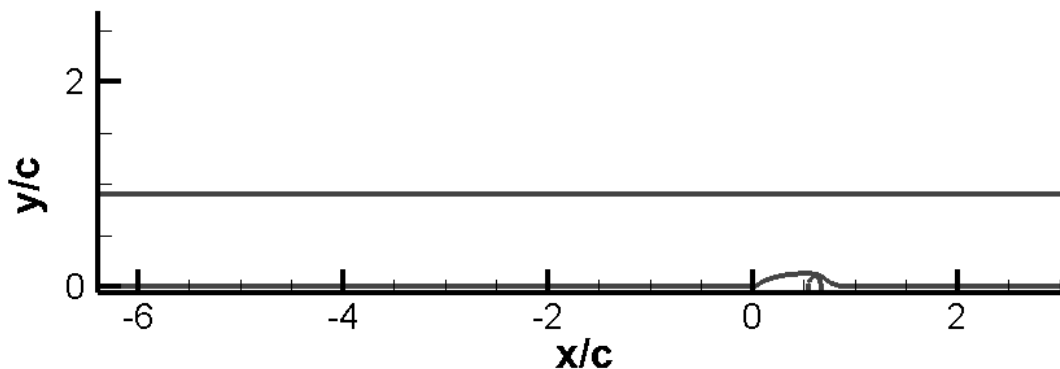


Figure 1: Computational domain for hump with oscillatory flow control

For the hump, the upstream inlet has been extended six times the chord to achieve the necessary boundary layer thickness over the hump as shown in figure 1. Pressure inlet, pressure outlet and symmetry boundary conditions of the solver are applied at inlet, outlet and top wall of the computational domain. A two-dimensional structured mesh with

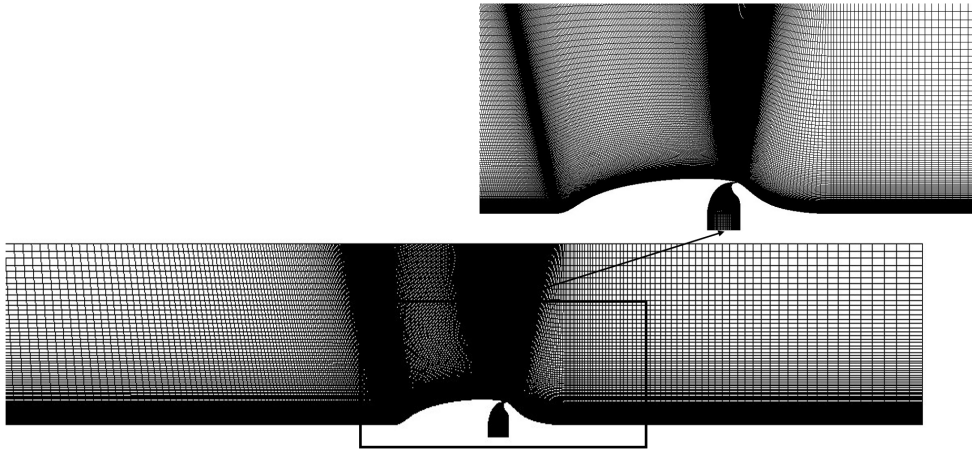


Figure 2: 2D structured mesh over the hump

about 700 points over the hump and 0.3 million total elements is generated. The mesh over the hump is shown in figure 2. A y^+ value less than 1 is used in both cases to have wall resolved flow.

2.3 Parametric study in hump with oscillatory control

Steady and unsteady RANS computations are carried out using Spalart Allmaras turbulence model. The physical time step of 10^{-5} seconds has been used in all cases and all unsteady computations have been initialized from converged steady simulation results.

Flow over the NASA hump model is simulated using steady and unsteady RANS model. The time averaged results from URANS give a very close match with the experimental case for the unforced case. Figure 3 shows the comparison of the time averaged coefficient of pressure (C_p) and coefficient of skin friction (C_f) from the URANS simulations with that of the experiment. The streamline plot from the separated region is shown in figure 4. It is observed that point of reattachment of the flow is at X/C of 1.2 compared to the experimental value of 1.1. A bias in surface pressure over the hump is observed due to the effect of end plates in the experiment which causes a local acceleration of flow. For the flow with no control, the experimental data is made available after temporarily removing the plates, but the data from different control cases are not corrected for this effect. Many CFD simulations have tried to modify the outer tunnel wall boundary to produce a converging wall effect which accelerates the flow and reduces this bias in pressure. However, since the interest of this work is on the simulation of synthetic jet characteristics effectively, this bias is ignored.

Experimental data pertaining to the flow control case reveals that as the jet momentum coefficient increases, the pressure recovery occurs much upstream and the separation bubble is shorter. It also showed that based on the reduced frequency, the jet characteristics shows two different behaviours. Introducing the synthetic jet with a frequency less than a reduced frequency of 0.77, showed an oscillation of wall pressure and faster recovery. URANS simulations were carried out to verify if these features are captured and are discussed in the sections below.

2.3.1 Effect of frequency of the jet

The jet was introduced at 65% of the chord as in experiments at a velocity of 26.6 m/s. Frequency and amplitude of piston motion are specified to match the velocity at jet exit with that in the experiments. Simulations were initialised using converged steady RANS results. The distance of point of reattachment from the jet exit location is calculated from the steady simulation. This is used to evaluate the frequency of a jet from the reduced frequency formulation. The standard test case frequency of the jet was evaluated to be around 115 Hz corresponding to a reduced frequency of 0.77. The surface pressure on the hump walls are time-averaged over 7-8 full cycles of oscillation to get the mean pressure distribution. The variation of C_p evaluated on the hump walls for various jet frequencies is shown in figure 5(a). The vertical shift in the experimental data is due to the effect of end-plates.¹¹ Earlier in figure 3, the experimental data with no flow control corrected for this effect is used to compare with the numerical results and a better match

SYNTHETIC JET CONTROL

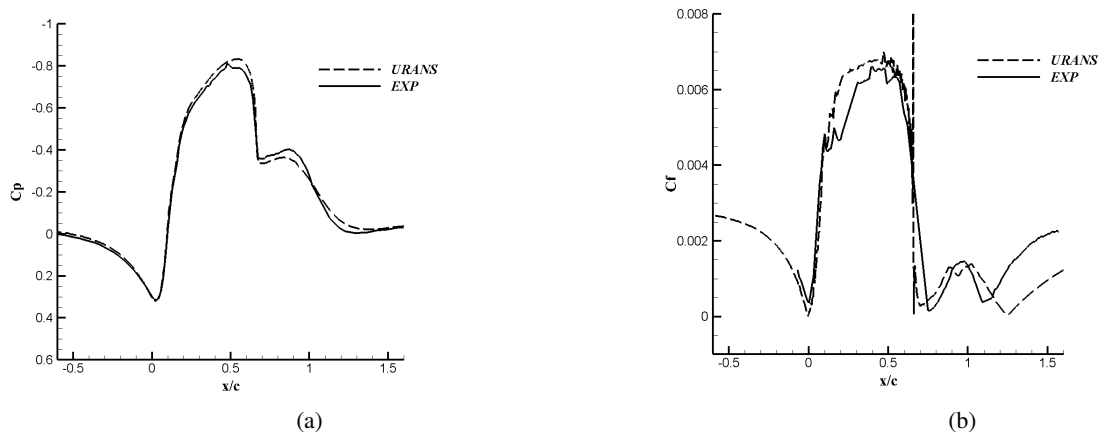
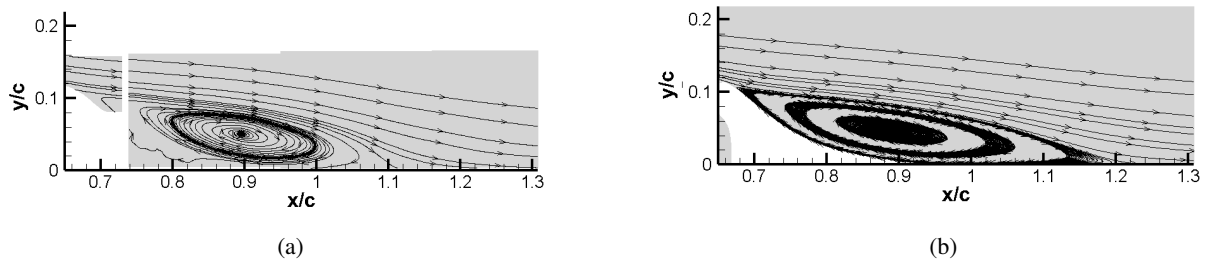
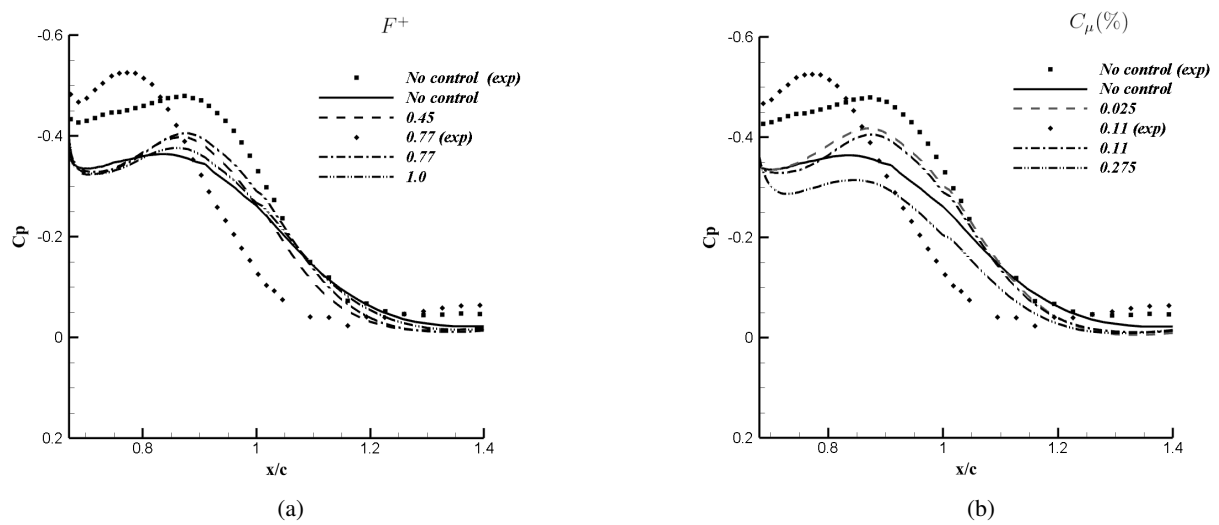
Figure 3: Time averaged profiles of a) coefficient of pressure (C_p) b) coefficient of skin friction (C_f) over the hump

Figure 4: Streamline plot a) PIV from experiment and b) URANS simulation

Figure 5: Mean streamwise pressure coefficients for various a) reduced frequencies for $C_\mu=0.11\%$ and b) reduced amplitudes for $F^+=0.77$

was observed. For the jet frequency of 115 Hz, the trend of surface pressure distribution on the wall matches the experimental data corresponding to the same reduced frequency. However, a faster pressure recovery rate is observed in the experiment compared to the simulations. For simulations with frequencies of 115 Hz or lower, there is an initial pressure drop before the recovery starts as in the experiment. For higher frequencies, this phenomenon is not observed in the simulations similar to experiments.

2.3.2 Effect of jet momentum coefficient

Jet momentum coefficient is a measure of the momentum of jet compared to the freestream. Effect of velocity of jet on the surface pressure distribution over the hump is simulated. All simulations were carried out for a jet frequency of 115 Hz. Figure 5(b) shows the variation of coefficient of pressure on the surface of hump for different velocities of the jet. With increase in the jet momentum, the bubble continues to shorten. It was observed that at lower velocities of jet, the fluctuations due to the periodic component is still the major effect on the separated region. But as the velocity increases, the strength of the separation bubble decreases, and the reattachment length reduces. The periodic perturbations are very minimal at this level, and the effect of frequency diminishes.

Thus, for an optimum case of flow control with synthetic jet, a combination of both the effects need to be considered. An optimum value needs to be defined for the velocity and frequency of the jet. The ability of CFD simulations to capture the different regimes of flow in cases of varying F^+ and C_μ is encouraging and the same was extended to the airfoil case of practical significance being considered as a candidate for STOL application.

3. Implementing the control for the high cambered wing section

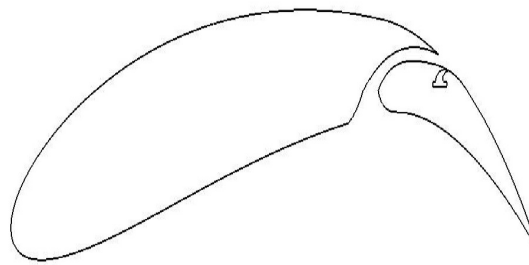


Figure 6: High cambered airfoil section(not to scale)

An unconventionally high cambered slotted airfoil with the slot placed at its maximum camber location shown in figure 6 is selected for implementing the synthetic jet control. The cavity is designed as a simple rectangular cavity for the ease of implementing the dynamic mesh model that was explained earlier in this paper. The throat width of the cavity is maintained at 0.2 percent of the chord and is embedded in the airfoil surface.

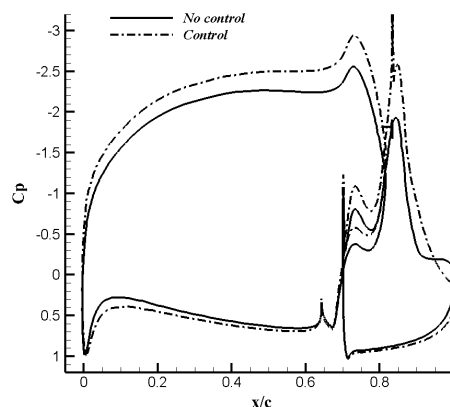


Figure 7: Comparison of coefficient of pressure with and without control

SYNTHETIC JET CONTROL

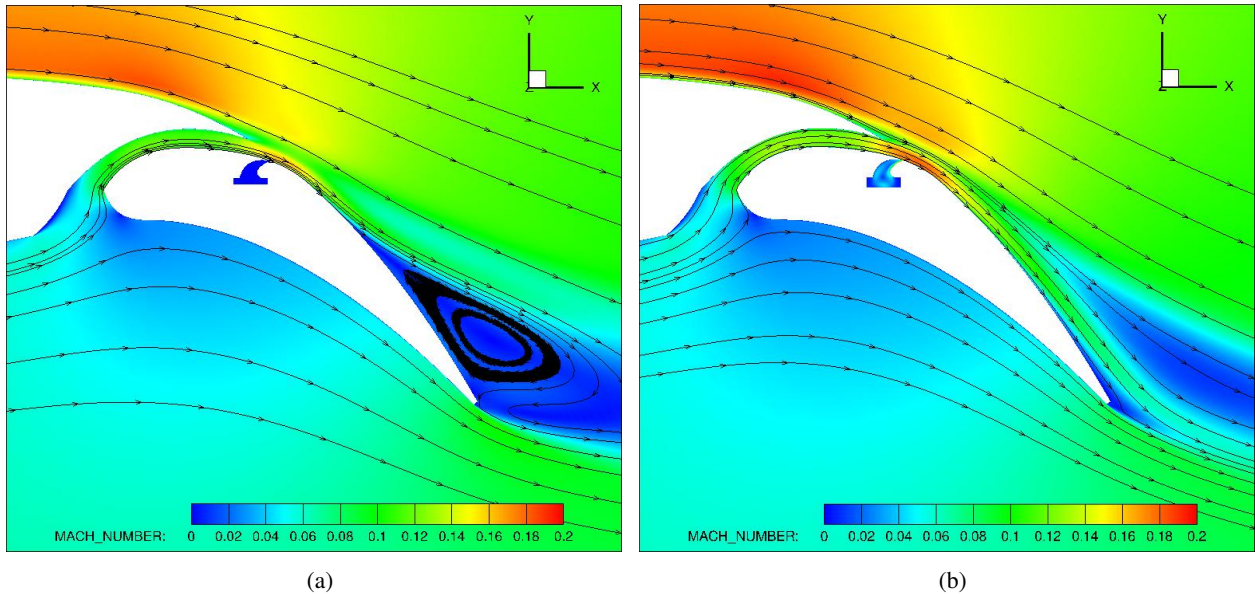


Figure 8: Mach contours and streamline plots around the trailing part of the airfoil design a) without control and b) with control $F^+=0.75$, $C_\mu=0.275$

3.1 Solution methodology

A circular domain of 100 chord is taken for the computation. Non-reflecting Riemann boundary condition is enforced on the far field and simulations are carried out at Mach number 0.1 at ambient pressure 101325 Pa at 4 degrees of angle of attack. A fine structured mesh with about 0.12 million volumes is generated for the studies presented. The control parameters are defined based on the bubble length evaluated from the steady RANS results of the 2D wing section. As per the discussions presented in the previous section, the parameters F^+ and a $C_\mu\%$ are chosen to be 0.75 and 0.275 respectively for effective control.

3.2 Results

The steady and unsteady simulations were carried out for the new configuration and 13 percent enhancement in lift is observed. The averaged coefficient of pressure for the control case is compared with the steady case in figure 7. Interestingly, the synthetic jet control by suppressing the separation bubble in the aft of the airfoil section effectively increases the flow turning resulting in improved lift over the entire section. Figure 8 shows the mach number contours around the airfoil with and without the jet control. It is observed that the choice of control parameters and the jet exit location has effectively suppressed the separation bubble and streamlined the flow.

4. Conclusions

The dynamic mesh model implemented in the hump with oscillatory control. With jet momentum coefficients greater than 0.11%, the pressure recovery improves though there is only minimal interaction of the periodic components with the separation bubble. Based on the study, reduced frequency of order less than one and jet momentum coefficient greater than one, has been used for the new airfoil control. With the addition of the synthetic jets, there is an improvement in the coefficient of lift for the wing configuration from the preliminary studies. Further studies are underway to optimize the jet location and realize a wing with control in the presence of propeller slip stream for STOL applications.

5. Acknowledgements

Special thanks to Dr. Munikrishna, CTO, S&I Engineering Solutions for assisting with the HiFUN solver, Mr. Sesa Sai, for his help in grid generation and other lab members for their insightful inputs. Authors also like to thank the SERC, IISc for providing with supercomputing time without which this work would have been difficult to complete.

References

- [1] https://turbmodels.larc.nasa.gov/other_exp_data/cfdval2004.
- [2] Smith B L and Glezer A. The formation and evolution of synthetic jets. *Physics of Fluids*, 10(9):2281â2297, 1998.
- [3] Glezer A and Amitay M. Synthetic jets. *Annu. Rev. Fluid Mech.*, (34):503â529, 2002.
- [4] Amitay M, Smith D R, Kibens V, Parekh D E, and Glezer A. Modification of the aerodynamics characteristics of an unconventional airfoil using synthetic jet actuators. *AIAA Journal*, 39(3):361–370, 2001.
- [5] Amitay M and Glezer A. Role of actuation frequency in controlled flow reattachment over a stalled airfoil. *AIAA Journal*, 40(2):209–216, 2002.
- [6] Traub L W, Miller A, and Rediniotis O. Effects of synthetic jet actuation on a rampingnaca 0015 airfoil. *Journal of aircraft*, 41(5):1153–1162, 2004.
- [7] P. R. Spalart and S. R. Allmaras. A one-equation turbulence model for aerodynamic flows. *AIAA Journal*, (92-0439), 1992.
- [8] Schaeffler N. W and Jenkins L. N. The isolated synthetic jet in crossflow: A benchmark for flow control simulation. *AIAA Journal*, page 2219, 2004.
- [9] Schaeffler N. W and Jenkins L. N. The isolated synthetic jet in crossflow: A benchmark for flow control simulation. *AIAA Journal*, 44(12):2846–2856, 2006.
- [10] Amsha S, O N Ramesh, and N Balakrishnan. Cfd simulation of synthetic jets. *Proceedings of Symposium on Applied Aerodynamics and Design of Aerospace Vehicle*, 2022.
- [11] Greenblatt D, Paschal K B, Yao C S, Harris J, Schaeffler N W, and Washburn A E. A separation control cfd validation test case, part 1: Baseline and steady suction. *AIAA Journal*, 44(12):2820–2830, 2006.
- [12] Greenblatt D, Paschal K B, Yao C S, and Harris J. A separation control cfd validation test case, part 2: Zero efflux oscillatory blowing. *AIAA Journal*, 44(12):2831–2845, 2006.
- [13] <https://sandi.co.in/>.
- [14] P.L. Roe. Approximate riemann solvers, parameter vectors, and difference schemes. *Journal of Computational Physics*, (135(2)), 1997.
- [15] V. Venkatakrishnan. Convergence to steady state solutions of the euler equations on unstructured grids with limiters. *Journal of Computational Physics*, (118), 1995.
- [16] Baum J. D. Luo, H. and R. Lohner. A fast matrix-free implicit method for compressible flows on unstructured grids. *Journal of Computational Physics*, 146, 1998.
- [17] Antony. Jameson. Time dependent calculations using multigrid, with applications to unsteady flows past airfoils and wings. *10th Computational Fluid Dynamics Conference*, 1991.
- [18] Dandois J, Garnier E, and P Sagaut. Unsteady simulation of synthetic jet in a crossflow. *AIAA Journal*, 44(2):225–238, 2006.
- [19] Xia H and Qin N. Detached-eddy simulation for synthetic jets with moving boundaries. *Modern Physics Letters B*, 19(28-29):1429–1434, 2005.